Continuous Low-Intensity Ultrasound Preserves Mitochondrial Potential, Inhibits NFκB Activation and Rescues Chondrogenesis of Mesenchymal Stromal Cells

Sarayu Bhogoju
The University of Alabama in Huntsville
Shahid Khan
The University of Alabama in Huntsville
Denzhi Wang
University of Alabama at Birmingham
Anuradha Subramanian (anu.subramanian@uah.edu)
The University of Alabama in Huntsville

Research

Keywords: Mesenchymal stromal cells (MSCs), Continuous low-intensity ultrasound (cLIUS), Chondrogenesis, NFκB pathway, Proinflammatory cytokines, Mitochondrial potential

Posted Date: April 2nd, 2021

DOI: https://doi.org/10.21203/rs.3.rs-342462/v1

Abstract

Objective: Dysregulation of the anabolic processes in a proinflammatory joint environment coupled with impeded chondrogenic differentiation of mesenchymal stromal cells (MSCs) led to inferior cartilage repair outcomes. The preponderance of proinflammatory cytokines activated nuclear factor kappa B (NFκB) and impeded the chondrogenesis of MSCs. Thus, strategies that minimize the deleterious effects of activated NFκB while promoting MSC chondrogenesis are of interest. The present study establishes the ability of continuous low-intensity ultrasound (cLIUS) to rescue MSC chondrogenesis impacted by a proinflammatory environment.

Methods: Human bone marrow-derived MSCs were seeded in alginate:collagen hydrogels and cultured for 21-days in an ultrasound-assisted bioreactor 14 kPa (5.0 MHz, 2.5 Vpp; 4-applications/day) for 21 days in the presence of IL1β and evaluated by qRT-PCR (n=10), immunofluorescence (n=15), western blotting (WB) (n=6), and immunohistochemistry (n=3). The differential expression of markers associated with NFκB pathway under cLIUS were evaluated upon a single exposure of cLIUS and assayed by qRT-PCR (n=3), immunofluorescence (n=30-60), WB (n=6) and tetramethylrhodamine methyl ester assay (n=50) was used to assess the mitochondrial potential under IL1β and cLIUS treatment.

Results: Chondroinductive potential of cLIUS was preserved as noted by the increased expression of SOX9 and deposition of collagen II. cLIUS extended its chondroprotective effects by stabilizing the NFκB complex in the cytoplasm via engaging the IκBα feedback mechanism, thus preventing its nuclear translocation. cLIUS acted as a mitochondrial protective agent by restoring the mitochondrial potential and the mitochondrial mRNA expression in a proinflammatory environment.

Conclusion: Our results demonstrated the potential of cLIUS for cartilage repair and regeneration under proinflammatory conditions.

Background

Damaged cartilage seldom heals; hence, therapies addressing restoration are of clinical relevance[1,2]. Strategies that rely on mesenchymal stromal cells (MSCs) to regenerate cartilage include mesenchymal-stromal-cell-implantation or microfracture and depend upon the in-situ differentiation of MSCs[3–5]. However, the inflamed environment caused by the surgical procedure itself or by the diseased joint[6] exerts a suppressive action on cartilage biosynthesis and the differentiation of MSCs into chondrocytes[7] and may explain inferior cartilage repair outcomes. Therapeutic measures that suppress the catabolic response in an inflamed environment by inhibiting key signaling mediators, including the nuclear factor kappa B (NFκB) pathway are required to enable effective repair processes.

Catabolic cytokines; interleukin-1beta (IL1β), tumor necrosis factor-alpha (TNFα), interleukin-6 (IL6), and interferon-gamma (IFNγ) were significantly elevated both in the synovial fluid and in the cartilage of diseased and operated joints[8]. IL1β and TNFα activated NFκB and its downstream targets (MMP13,

ADAMTS4/5) inhibited the biosynthesis of the cartilage matrix[9]. Activated NFκB also downregulated the expression of SOX9, the master regulator of chondrogenesis[10]. Not surprisingly, MSC chondrogenesis in pellet and 3D cultures were adversely impacted by the use of cytokines[11–14] and, the gene delivery of IL1RA, culture additives like magnesium, melatonin, and curcumin were shown rescue impaired MSC chondrogenesis[15–18].

Low-intensity continuous ultrasound (cLIUS) when employed at 14 kPa (5 MHz and 2.5 Vpp) was shown to be a positive regulator of chondrogenesis *in vitro*[19,20]. Further, the chondroprotective effects of cLIUS (14 kPa) against proinflammatory cytokines on intact cartilage explants was demonstrated where cytokine-induced increases in NFκB expression and its downstream targets were suppressed, and the expression of COLII and TIMP1 genes were upregulated[21]. Recently the chondroinductive ability of cLIUS (14 kPa) was demonstrated in the absence of exogenously added growth factors[19,20,22].

As most early *in vivo* cartilage reparative processes occur in an inflammatory environment; thus, this work focuses on evaluating the ability of cLIUS to mitigate the impairment of MSC chondrogenesis in a proinflammatory environment. Therefore, the assessment of MSC chondrogenesis in 3D hydrogels under cLIUS, in the presence of IL1β was undertaken, where MSCs seeded in alginate:collagen hydrogels were cultured in the ultrasound-assisted bioreactor for 21 days and evaluated by quantitative real-time polymerase chain reaction (qRT-PCR), immunofluorescence (IF), western blotting (WB) and immunohistochemistry. To quantify the NFκB pathway markers under cytokines and their differential expression under cLIUS, MSCs were subjected to a single exposure of cLIUS, and outcomes were evaluated by qRT-PCR, IF and WB. The ability of cLIUS to reverse the cytokine-induced impairment of mitochondrial potential (ΔYm) was measured by tetramethylrhodamine methyl ester (TMRM) assay.

Materials And Methods

Cell culture

Bone marrow-derived human MSCs (male, age 38) were purchased from Lonza (Walkersville, MD, USA) and expanded as previously reported[19]. Passage 3 to 5 MSCs were trypsinized and employed in all experiments. All cell culture experiments were carried out in humidified incubators at 37ºC with 5% CO_2. The study design adopted is schematically shown in Figure 1.

Preparation and encapsulation of MSCs in 3D hydrogels

MSCs were encapsulated in alginate:collagen hydrogels at a seeding density of 2 x 10^5 cells per hydrogel and cultured for 21 days with and without IL1β (R&D systems, 201-IL) or cLIUS stimulation. Briefly, a 0.4% sterile collagen solution (Advanced BioMatrix, 5153) was mixed with neutralizing solution (Advanced BioMatrix, 5155) as per the manufacturer's instructions. MSCs were added to the neutralized collagen solution at a ratio of 5:1 and mixed with 2% sterile alginate (Sigma, W201502) to yield a final concentration of 1.2% (alginate) and 0.11% (collagen). 100µl of the alginate-collagen-MSCs solution was

pipetted into 5 x 5 mm agarose molds containing 0.5 M $CaCl_2$ and incubated at 37ºC for 30 min. Formed hydrogels were removed and cultured in six-well tissue culture plates (TCPs) in α-MEM basal media supplemented with 10% fetal bovine serum, 1x Glutamax™ and 1x Antibiotic- Antimyotic™ (Gibco, USA) solution for 72 hr.

MSCs culture in hydrogels and cLIUS treatment

Hydrogels were divided into four sample groups as: Group 1: cLIUS (-), IL1β (-); Group 2: cLIUS (+), IL1β (-); Group 3: IL1β (+), cLIUS (-) and Group 4: IL1β (+) cLIUS (+), and schematically depicted in Figure 1. Media was replaced every 3 days, where only half of the media was supplemented with fresh media containing 10 ng/ml of IL1β. Automated cLIUS stimulation was applied using the bioreactor developed at the University of Alabama in Huntsville (UAH) at the following regimen: 14 kPa (5.0 MHz, 2.5 Vpp), 10 min/application, and four applications/day. Hydrogels were retrieved at the end of 21 days and subjected to outcome analysis as listed in Figure 1.

MSCs culture in monolayer and cLIUS treatment

MSCs were plated in 6-well or 12-well TCP at the following seeding densities: 2 x 10^5 or 5 x 10^4 cells/well (protein and RNA extractions following treatment with cytokines and non-treated controls) and 1 x 10^4 cells/coverslip (CS) (for TMRM assay and IF studies following treatment with cytokines and non-treated controls). All treatments with cytokines and/or cLIUS were conducted after 48 hr of initial seeding of MSCs in TCP or CS. All cytokines were purchased from R&D systems (Minneapolis, MN) and were employed at a concentration of 10 ng/ml. Non-focused immersion transducers (Panametrics V300, 12.7 mm diameters, Panametrix, Waltham, MA, USA) were used to apply cLIUS to plated MSCs using procedure detailed elsewhere[21]. MSCs were exposed to cytokines and cLIUS was applied one time for 10 or 20 min at 5 MHz (2.5 Vpp) with constant pressure amplitude of 14 kPa. In addition to qRT-PCR following cLIUS stimulation, WB, TMRM assay and IF staining were conducted.

Cell viability assay

Cell viability in hydrogels was assessed by Live/Dead™ Viability/Cytotoxicity kit (Molecular Probes, USA) according to manufacturer's instructions[21] and visualized with the Zeiss LSM 700 Confocal Microscope. All the images were collected at 10x magnification (z step size = 12 μm).

Histology and Immunohistochemistry

Hydrogels were fixed using a protocol listed elsewhere[23,24] and used for histological and immunohistochemical analysis (n=3) at the pathology core research laboratory, University of Alabama in Birmingham (UAB). 8 mm sections were stained using hematoxylin and eosin (H&E) and immunostained with 1:20 dilution of Collagen II (COLII) antibody (Abcam, 34712) with corresponding secondary antibody. A human bone section was included as a positive control.

Quantitative real-time PCR (qRT-PCR)

MSCs were released from hydrogels (n=10) using the dissolution buffer (DB) (55 mM sodium citrate, 50 mM EDTA, and 90 mM NaCl, pH 6.9) and homogenized with the Trizol reagent (Invitrogen, USA). In monolayer studies, cells from TCP plates were homogenized with 300µl of Trizol reagent per well. Homogenates from two wells served as one replicate, and three such replicates were used for gene expression analysis (n = 3). RNA was extracted using PureLink RNA Mini Kit (Thermofisher, USA). The qRT-PCR analysis was carried out using QuantStudio 3 real-time PCR system (Applied Biosystems, USA) employing TaqMan® RNA-to-CT™ 1-Step Kit (Life Technologies, USA).

TaqMan® Gene expression assays (Life Technologies, USA) used are as follows:

GAPDH (Hs02786624_g1), MMP13 (Hs00942584_m1), ADAMTS4 (Hs00192708_m1), NFκB (Hs00765730_m1), TIMP1 (Hs01092512_g1), SOX9 (Hs00165814_m1), RUNX2 (Hs01047973_m1), PPARG (Hs01115513_m1) and MTCO3 (Hs02596866_g1), MTCYB (Hs02596867_s1). The expression of mRNA transcripts was normalized to GAPDH expression and relative expression levels were calculated using the $2^{-\Delta\Delta Ct}$ method.

Immunofluorescence staining

MSCs on CS were fixed in 4% paraformaldehyde (4% PFA) for 20 min and blocked with 2% goat serum in 1X TBST (Tris buffer saline with 0.1% tween20) blocking buffer (BB) for 2 hr. CS were then incubated with 1:1000th diluted rabbit anti-phospho-NFκB p65 monoclonal antibody (Invitrogen, MA5-15160) in BB overnight at 4ºC. Upon washing, CS were incubated with 1:1000th diluted goat anti-rabbit IgG H&L conjugated with Alexa flour 488 (Abcam, 150077) for 1 hr at room temperature (RT) and mounted on a glass slide with DAPI mounting media (ProLong™ Diamond Antifade Mountant with DAPI, P36962). For CS subjected to double IF staining, CS treated as above till the NFκB detection step and then washed and blocked with BB for 1 hr at RT and incubated with 1:1000th diluted rabbit anti-human SOX9 Mab (CST, 82630) overnight at 4^{o}C. Upon washing, CS were incubated with 1:1000th diluted goat anti rabbit IgG H&L conjugated with Alexa flour 594 (CST, 8889S), for 1 hr at RT and mounted as mentioned earlier. All images were captured using the Zeiss LSM 700 confocal microscope at 63x magnification. Fluorescent intensities were quantified using ImageJ^{TM} software (n=30-60).

To visualize pNFκB and COLII in hydrogels, a modified IF staining protocol was adopted[25] where hydrogels were washed in HBSSCM (HBSS containing 1.26 mM $CaCl_2$ and 0.4 mM $MgSO_4$) and fixed with 4% PFA containing 1.26 mM $CaCl_2$, 400 mM $MgSO_4$ for 60 min. After copious washing, samples were permeabilized with 0.1% Triton X-100 in HBSSCM and blocked with BB (5% BSA, 10% goat serum in HBSSCM containing 0.2% tween) for 2 hr at RT. pNFκB and COLII were independently stained and detected as mentioned earlier. COLII was detected using 1:1000th diluted rabbit anti-human collagen II polyclonal antibody (Abcam, 34712) and Alexa flour 488 conjugated goat anti rabbit polyclonal antibody. All images were collected at 63x magnification using the Zeiss LSM 700 confocal microscope (z stacks:

180-190μm and z step size: 5μm), and fluorescent intensity was quantified using ImageJ™ software (n=15).

Protein isolation and Western Blotting

Total protein was extracted and quantified upon cessation of cLIUS stimulation using previously published methods[22]. Lysates from three independent wells were pooled together for total protein extraction (n=6). SDS-PAGE was conducted using Novex™ Tris-Glycine gels (Invitrogen, USA) per the manufacturer's instructions. Proteins separated by SDS-PAGE were transferred to the PVDF membrane. Membranes were blocked with 5% dry milk (CST,9999) for 1 hr at RT and incubated with 1:1000th diluted primary antibodies of pNFκB (CST, 3033), tNFκB (CST, 8242), pIκBα (CST, 2859), and tIκBα (CST, 4814) in 5% BSA overnight at 4^{o}C. Detection was performed by incubating with 1:2000th diluted horse-radish-peroxidase (HRP) labeled secondary antibodies to rabbit IgG (CST, 7074) and mouse IgG (CST, 7076), β-actin was used as a loading control. The cytoplasmic and nuclear fractions were isolated using NE-PER™ kit (Thermo Scientific, USA) and processed for western blotting as described.

To quantify COLII expression levels in hydrogels (n=6), MSCs were released using DB and total protein was extracted and quantified as detailed elsewhere[22]. Proteins were separated, transferred and blocked and membranes were incubated with 1:1000th diluted COLII antibody (Abcam, 34712) overnight at 4^{o}C. Membranes were washed and incubated with HRP labeled secondary antibody rabbit IgG for 2 hr at RT and β-actin was used as a loading control. All blots were visualized by incubating with Clarity™ western ECL kit (Bio-Rad, USA) as per the manufacturer's instructions. Images were captured with a ChemiDoc MP imaging system (Bio-Rad, USA), and the band intensities were quantified using ImageJ™ software.

Measurement of Mitochondrial Potential using TMRM assay

Mitochondrial potential(ΔYm) in various study groups (Figure 1) was assessed using the TMRM assay as per manufacturer's instructions. Briefly, cells on CS were washed and incubated with 100nM TMRM reagent for 30 min. Live images were captured using Zeiss LSM 700 confocal microscope at 10x magnification, and fluorescent intensity was quantified using ImageJ™ software (n=50).

Statistical Analysis

The data are expressed as average ± standard deviation. For qRT-PCR, monolayer IF, and mitochondrial potential data analyses, one-way ANOVA followed by post-hoc Sidak's multiple comparison test was used. One-way ANOVA with post-hoc Dunnett's multiple comparison test was used to analyze data collected from western blot and hydrogel IF. The graphs were generated using GraphPad Prism software. Statistical significance was established as follows: $p<0.05$ (denoted as *), $p<0.01$ (denoted as **), $p<0.001$ (denoted as ***), $p<0.0001$ (denoted as ****).

Results

The ability of cLIUS to rescue and promote MSC chondrogenesis in the presence of proinflammatory cytokines was evaluated. Cellular viability was assessed on day 21 by Live-Dead^{TM} assay and shown in Additional file.1: Figure S1. Good cell viability was observed in all study groups, no appreciable levels of dead cells (red) were observed.

cLIUS promotes collagen II deposition

The expression of COLII protein in hydrogels was analyzed by western blotting, quantified, and shown in Figures 2A and 2B. Low levels of COLII expression was noted in controls (group 1), and in IL1β treated hydrogels (group 3). A 77-fold higher expression of COLII was observed in hydrogels stimulated with cLIUS in the presence of IL1β (group 4) compared to groups 1 and 3.

Hydrogels were stained for COLII for direct visualization by IF, quantified, and presented in Figure 3C. Fold-increases observed with IF were in agreement with the trends noted by western blotting.

Histological and immunohistochemical analysis

H&E stained sections showed similar cellularity in all study groups (data not shown). Immunohistochemical staining for COLII in alginate-collagen hydrogels is shown in Figure 2C. Compared to IL1β treated hydrogels (group 3), a darker COLII stain was noted in samples, which additionally received cLIUS (group 4). IHC analyses were confirmed by western blotting for COLII and shown in Figure 2A.

cLIUS attenuates NFκB and upregulates SOX9 gene expression in hydrogels

Gene expression of catabolic markers (NFκB, MMP13, ADAMTS4) and lineage markers (RUNX2, PPARγ, and SOX9) was evaluated by qRT-PCR and shown in Figure 3A. The presence of IL1β (group 3) significantly elevated the gene expression of MMP13 (3.6fold) and NFκB (3.4fold) when compared to controls (group 1). cLIUS stimulation (group 4) significantly diminished IL1β induced upregulation of these markers. Similar to previous results,[22] a 20-fold upregulation in the expression of SOX9, the primary chondrogenic transcription marker, was noted under cLIUS compared to controls. Treatment with IL1β downregulated the gene expression of SOX9 (group 3). In contrast, a 15-fold higher expression of SOX9 was noted in group 4, where IL1β treated samples were exposed to cLIUS. Interestingly, low gene expression levels of osteogenic and adipogenic markers (RUNX2 and PPARγ) were noted in cLIUS stimulated samples with or without IL1β treatment.

cLIUS abrogates pNFκB nuclear translocation in 3D scaffolds

The effect of cLIUS on the localization and nuclear translocation of phosphorylated NFκB was evaluated in hydrogels through IF and presented in Figure 3B. Compared to the control (group 1), a 38-fold higher level of pNFκB intensity in the cytoplasm was noted in IL1β treated samples (group 3). The application of cLIUS, in the presence of IL1β (group 4), decreased the cytoplasmic pNFκB intensity to levels observed in group 1. The inclusion of IL1b led to enhanced localization of pNFκB in the nucleus when compared to

controls. cLIUS stimulation (group 4) diminished the intensity of pNFκB in the nucleus to levels observed in controls, indicating that cLIUS blunted the translocation of pNFκB to the nucleus in the presence of IL1β.

As molecular consequences following cLIUS on the canonical NFκB pathway markers are best evaluated upon a single exposure of cells to cLIUS in monolayer experiments, MSCs in monolayers were subjected to study design shown in Figure 1.

cLIUS downregulates catabolic and upregulates anabolic gene expression

The gene expression levels of catabolic (MMP13, ADAMTS4), anabolic (TIMP1), and transcription markers (NFκB and SOX9) were evaluated by qRT-PCR and shown in Figure 4A. In the presence of IL1β (group 3), the expression of catabolic genes and NFκB was significantly elevated, and the gene expression of SOX9 and TIMP1 were downregulated compared to controls (group 1). When IL1β treated cells were further exposed to cLIUS, an abrogation in the expression levels of catabolic genes to basal levels, similar to group 1, was noted. However, in the same sample treatment (group 4), cLIUS yielded comparable gene expression levels of SOX9 and TIMP1 to group 2. Independent experiments were also carried out in the presence of TNFα or IL6 and similar trends were noted and presented in Figure 4B and 4C. Cumulative results demonstrated that cLIUS promotes the gene expression of anabolic markers in the presence of proinflammatory cytokines by downregulating catabolic genes MMP13, ADAMTS4, and NFκB.

cLIUS rescinds NFκB and promotes SOX9 localization to the nucleus

To evaluate the influence of cLIUS on IL1β-induced cellular localization of pNFκB, IF studies were undertaken and presented in Additional file.2: Figure S2A. As expected, the presence of IL1β (group 3) yielded a 21-fold higher intensity of pNFκB in the cytoplasm and nuclear region when compared to controls (group 1). The cytoplasmic and nuclear intensity levels of pNFκB were significantly diminished when cells were exposed to cLIUS stimulation in the presence of IL1β (group 4). Comparable trends were noted when experiments were undertaken in the presence of TNFα or IL6 (Additional file.2: Figure S2B and S2C).

As the nuclear localization of pNFκB is linked to its proinflammatory transcriptional activity, localization of pNFκB and SOX9 in the cytoplasmic and nuclear regions were visualized by double IF, and the fluorescent intensities were quantified and presented in Figure 5. The presence of IL1β reduced the levels of SOX9 in the nucleus (group 3) when compared to group 2. However, cLIUS stimulation in the presence of IL1β (group 4) inverted the localization of these markers, where the levels of nuclear pNFκB were decreased, and SOX9 was upregulated. Similar trends were observed with cytoplasmic levels of pNFκB and SOX9. These results indicate the ability of cLIUS to maintain the expression of SOX9, the main transcription factor of COL2A1, in the presence of proinflammatory cytokines.

cLIUS minimizes pNFκB expression and persuades total IκBα expression

To ascertain the effect of cLIUS on the markers of the NFκB pathway, protein expression of phosphorylated NFκB (pNFκB), total NFκB (tNFκB), phosphorylated IκBα (pIκBα), and total IκBα (tIκBα) was analyzed by western blotting and shown in Figure 6. In IL1β, treated samples (group 3), a 26-fold higher level of pNFκB expression and a 126-fold elevated level of pIκBα expression was observed in comparison to non-treated controls (group 1). The expression level of tIκBα was significantly downregulated in the presence of IL1β (indicated by the blue arrow in Figure 6A). However, cLIUS stimulation (group 4) diminished the IL1β upregulated expression of these transcription factors to control levels. Notably, when IL1β treated cells were exposed to cLIUS (group 4), the expression level of tIκBα was similar to that observed in controls (indicated by the red dotted lines in Figure 6A). The expression of total tIκBα and pNFκB in the cytoplasmic and nuclear fractions were also assessed and shown in Additional file.3: Figure S3. The elevated levels of tIκBα were noted in both fractions in samples from group 4. The significant increase in tIκBα expression levels indicates cLIUS-induced suppression of the NFκB pathway in the presence of IL1β by engaging the tIκBα feedback mechanism, thus rescuing MSCs from negative impacts of activated NFκB.

cLIUS acts as a mitochondrial protective agent

There is increasing evidence for the presence of NFκB in the mitochondria of cells that are exposed to cytokines and has been shown to lower the ΔYm[26]. TMRM assay was employed to ascertain the ΔYm under cLIUS and in the presence of IL1β, and both the fluorescent images and their quantification are shown in Figure 7. cLIUS alone (group 2) had no discernable impact on ΔYm when compared to controls (group 1). This is supported by our previous observation that cLIUS regimens employed in this study do not generate reactive oxygen species[27]. As expected, the ΔYm was significantly downregulated in IL1β treated samples (group 3) as compared to controls (group 1). The IL1β induced decrease in ΔYm was reinstated by cLIUS stimulation (group 4) as demonstrated by a significant ($p<0.0001$) increase in ΔYm (Figure 7B).

Previously, the presence of NFκB in mitochondria was noted to lower the expression of Cytochrome c oxidase Ⅲ (COXIII) and Cytochrome b (CYB)[26]. Thus, gene expression of COX Ⅲ and CYB mRNA levels were used as an indirect measure of the NFκB in the mitochondria and evaluated by qRT-PCR and presented in Figure 7C. In the presence of IL1β (group 3), both COX Ⅲ and CYB levels were decreased when compared to controls (group 1). When IL1β treated cells were exposed to cLIUS (group 4), the gene expression levels of COXIII and CYB were unregulated, as noted in controls.

Discussion

It is well-established that IL1β and TNFα are upregulated in diseased and operated joints and exert catabolic effects via the canonical and non-canonical NFκB pathways[11]. Cytokine induced activation of NFκB downregulated the key chondrogenic transcription factor, SOX9 and upregulated the expression of matrix-degrading proteins (MMP13, ADAMTS4),[28,29] thus impeding chondrogenesis. Therefore, the resulting imbalance of the anabolic processes in a proinflammatory environment inhibits MSC

chondrogenesis leading to inferior cartilage repair outcomes. Hence, strategies to rescue MSC chondrogenesis under proinflammatory conditions are of interest. In that regard, select natural compounds with known anti-inflammatory properties were shown to rescue MSC chondrogenesis in the presence of IL1β; by suppressing the activation of NFκB and maintaining the expression of chondrocyte markers[15,18]. Similarly, delivery of siRNA, the addition of divalent ions, and hypoxic culture conditions helped rescue chondrogenesis of MSCs in a proinflammatory environment by suppressing the activation of NFκB[11,16,30].

The ability of ultrasound to promote MSC chondrogenesis was demonstrated, and mainly conducted in the absence of cytokines[19,22]. To the best knowledge, this is the first report that demonstrated the ability of cLIUS to abrogate the deleterious impact of IL1β and rescue MSC chondrogenesis by maintaining elevated levels of COLII while downregulating the activity of NFκB. In the present study, increased nuclear deposition of SOX9 and its elevated gene expression in the presence of IL1β indicates the chondroinductive ability of cLIUS. cLIUS further extended its chondroinductive potential by down regulating the cytokine (IL1β, TNFα and IL6) induced catabolic responses (MMP13, ADAMTS4 and NFκB) and upregulating anabolic responses (SOX9, TIMP1) irrespective of cytokines tested in this study.

Under inflammatory conditions, NFκB is the main transcription factor that induces the expression of catabolic genes,[28,29] strategies that aim to rescue MSC chondrogenesis are typically focused on the canonical pathways of NFκB activation. In normal cells, the NFκB complex exists in the cytoplasm as an NFκB dimer bound to its inhibitor protein tIκB, which impedes NFκB DNA-binding activity and prevents its nuclear translocation. In the presence of inflammatory stimuli, signal-dependent phosphorylation of NFκB and IκB proteins led to the dissociation of the NFκB complex and the subsequent nuclear translocation of the NFκB dimer that induced the transcription of inflammatory genes. Phosphorylated IκBα is then designated for ubiquitination and degradation[31]. In the present study, as anticipated, the inclusion of IL1β in the culture led to increased levels of pNFκB and pIκBα, indicating increased activity of IKK[31] with a concomitant reduction of tIκBα levels. cLIUS blunted the expression of pNFκB and pIκBα, indicating reduced IKK activity. Surprisingly cLIUS restored the levels of tIκBα. Low levels of pIκBα and high levels of tIκBα in group 4 samples indicated that, the NFκB complex is stabilized under cLIUS by hindering the IκBα phosphorylation. The elevated levels of tIκBα observed in the cytoplasm and nuclear fractions denotes that cLIUS engages the tIκBα mediated feedback mechanism both in the cytoplasm and nucleus. This study documents the ability of cLIUS to rescue MSC chondrogenesis by downregulating NFκB activity via the IκBα assisted negative feedback regulation.

Chondrocytes, when exposed to proinflammatory cytokines (i.e., IL1β, TNFα) *in vitro* as in an osteoarthritic joint environment, showed a reduction in enzyme mitochondrial activities of complexes II and III, as well as a reduction in ΔYm[26]. In particular, the expression of mitochondrially encoded COX and CYB mRNAs was reduced by cytokines[26]. When the activation of mitochondrial NFκB was inhibited by the expression of the super-repressor form of IκBα, expression of both COX III and CYB mRNA returned to normal levels[26]. These data indicate that the NFκB regulatory pathway exists in mitochondria and that

NFκB levels can be negatively correlated to mitochondrial mRNA expression. Thus, mRNA levels of COX III and CYB were used as an indirect indication of the presence of NFκB in the mitochondrion when treated with cytokines[26]. As anticipated, our results showed that in IL1β treated samples, expression of both COX III and CYB mRNA were downregulated when compared to controls as well the ΔYm was reduced, alluding to the presence of NFκB in the mitochondria. Interestingly, cLIUS acts as a mitochondrial protective agent where it restores both the ΔYm and the mRNA levels of COX III and CYB). To our knowledge, mitochondrial protective ability of cLIUS has not previously reported. It is possible that cLIUS blunts the translocation of pNFκB to the mitochondria, or it abolishes the activity of pNFκB in the mitochondria. These aspects will be investigated in greater detail in our ongoing investigations.

Conclusions

In summary, this study reinforces the ability of cLIUS to rescue MSC chondrogenesis in a proinflammatory environment by inhibiting the nuclear translocation of NFκB by taking advantage of the IκBα feedback mechanism as well as protecting the mitochondrial potential and mitochondrial mRNA expression (Figure 8). Future studies will focus on the in-depth evaluation of mitochondrial dynamics under cLIUS in a proinflammatory environment. This study establishes the potential of cLIUS to improve and enhance outcomes of *in vivo* cartilage repair therapies. Translation of promising *in vitro* findings with cLIUS requires an understanding of the cLIUS propagation in the joint space along with optimal transducer settings. Current efforts are focused on establishing relevant mathematical models to allow for translation to small animal cartilage repair models to demonstrate the utility of cLIUS to improve cartilage repair outcomes.

Abbreviations

cLIUS: Continuous low-intensity ultrasound; COLII: Collagen II; COX Ⅱ: Cytochrome c oxidase Ⅱ; CYB: Cytochrome b; IF: Immunofluorescence; IL1β: Interleukin-1beta; IL6: Interleukin-6; MSCs: Mesenchymal stromal cells; NFκB: Nuclear factor kappa B; qRT-PCR: Quantitative real-time polymerase chain reaction; SOX9: Sex determining region Y-box 9; TMRM: tetramethylrhodamine methyl ester; TNFα: Tumor necrosis factor-alpha; WB: Western blotting; ΔYm: Mitochondrial potential.

Declarations

Ethics approval and consent to participate

Not applicable

Consent for publication

Not applicable

Availability of data and material

All data generated or analyzed during this study are included in this published article (and its supplementary information files).

Funding

The research sources are from National Health Institute grants (1R21EB025921-01A1 and 1R03AG062730-01).

Competing Interests

The authors declare they have no competing interests.

Author's contributions

AS, SB planned and designed the study. SB carried out experiments, analyzed and interpreted data. SK helped in experiments and data representation. AS and SB drafted the manuscript. All authors revised and approved the final version of the manuscript.

Acknowledgments

We thank Dr. Ahmad Lawan from the Biology department at the University of Alabama in Huntsville, for using the ChemiDoc MP imaging system. Troubleshooting efforts of Mr. Thor Wilson with the bioreactor were invaluable. We want to acknowledge Dr. N. Sahu at Stanford University for her critical inputs.

References

1. Orth P, Rey-Rico A, Venkatesan JK, Madry H, Cucchiarini M. Current perspectives in stem cell research for knee cartilage repair. *Stem Cells Cloning Adv Appl*. 2014;7(1):1-17. doi:10.2147/SCCAA.S42880
2. Gao J, Yao JQ, Caplan AI. Stem cells for tissue engineering of articular cartilage. *Proc Inst Mech Eng Part H J Eng Med*. 2007;221(5):441-450. doi:10.1243/09544119JEIM257
3. Martín AR, Patel JM, Zlotnick HM, Carey JL, Mauck RL. Emerging therapies for cartilage regeneration in currently excluded 'red knee' populations. *npj Regen Med*. 2019;4(1). doi:10.1038/s41536-019-0074-7
4. Steinert AF, Rackwitz L, Gilbert F, Nöth U, Tuan RS. Concise Review: The Clinical Application of Mesenchymal Stem Cells for Musculoskeletal Regeneration: Current Status and Perspectives. *Stem Cells Transl Med*. 2012;1(3):237-247. doi:10.5966/sctm.2011-0036
5. Filardo G, Vannini F, Marcacci M, et al. Matrix-assisted autologous chondrocyte transplantation for cartilage regeneration in osteoarthritic knees: Results and failures at midterm follow-up. *Am J Sports Med*. 2013;41(1):95-100. doi:10.1177/0363546512463675
6. Kondo M, Yamaoka K, Tanaka Y. Acquiring chondrocyte phenotype from human mesenchymal stem cells under inflammatory conditions. *Int J Mol Sci*. 2014;15(11):21270-21285. doi:10.3390/ijms151121270

7. Lolli A, Colella F, De Bari C, van Osch GJVM. Targeting anti-chondrogenic factors for the stimulation of chondrogenesis: A new paradigm in cartilage repair. *J Orthop Res*. 2019;37(1):12-22. doi:10.1002/jor.24136
8. Tsuchida AI, Beekhuizen M, 't Hart MC, et al. Cytokine profiles in the joint depend on pathology, but are different between synovial fluid, cartilage tissue and cultured chondrocytes. *Arthritis Res Ther*. 2014;16(1):1-15. doi:10.1186/s13075-014-0441-0
9. Wojdasiewicz P, Poniatowski ŁA, Szukiewicz D. The role of inflammatory and anti-inflammatory cytokines in the pathogenesis of osteoarthritis. *Mediators Inflamm*. 2014;2014. doi:10.1155/2014/561459
10. Sitcheran R, Cogswell PC, Baldwin AS. NF-κB mediates inhibition of mesenchymal cell differentiation through a posttranscriptional gene silencing mechanism. *Genes Dev*. 2003;17(19):2368-2373. doi:10.1101/gad.1114503
11. Wehling N, Palmer GD, Pilapil C, et al. Interleukin-1β and tumor necrosis factor α inhibit chondrogenesis by human mesenchymal stem cells through NF-κB-dependent pathways. *Arthritis Rheum*. 2009;60(3):801-812. doi:10.1002/art.24352
12. Zayed MN, Schumacher J, Misk N, Dhar MS. Effects of pro-inflammatory cytokines on chondrogenesis of equine mesenchymal stromal cells derived from bone marrow or synovial fluid. *Vet J*. 2016;217:26-32. doi:10.1016/j.tvjl.2016.05.014
13. Jagielski M, Wolf J, Marzahn U, et al. The influence of IL-10 and TNFα on chondrogenesis of human mesenchymal stromal cells in three-dimensional cultures. *Int J Mol Sci*. 2014;15(9):15821-15844. doi:10.3390/ijms150915821
14. Kondo M, Yamaoka K, Sonomoto K, et al. IL-17 inhibits chondrogenic differentiation of human mesenchymal stem cells. *PLoS One*. 2013;8(11). doi:10.1371/journal.pone.0079463
15. Gao B, Gao W, Wu Z, et al. Melatonin rescued interleukin 1β-impaired chondrogenesis of human mesenchymal stem cells. *Stem Cell Res Ther*. 2018;9(1):1-12. doi:10.1186/s13287-018-0892-3
16. Hu T, Xu H, Wang C, Qin H, An Z. Magnesium enhances the chondrogenic differentiation of mesenchymal stem cells by inhibiting activated macrophage-induced inflammation. *Sci Rep*. 2018;8(1):1-13. doi:10.1038/s41598-018-21783-2
17. Armbruster N, Krieg J, Weißenberger M, Scheller C, Steinert AF. Rescued chondrogenesis of mesenchymal stem cells under interleukin 1 challenge by foamyviral interleukin 1 receptor antagonist gene transfer. *Front Pharmacol*. 2017;8(MAY):1-15. doi:10.3389/fphar.2017.00255
18. Buhrmann C, Mobasheri A, Matis U, Shakibaei M. Curcumin mediated suppression of nuclear factor-κB promotes chondrogenic differentiation of mesenchymal stem cells in a high-density co-culture microenvironment. *Arthritis Res Ther*. 2010;12(4). doi:10.1186/ar3065
19. Thakurta SG, Budhiraja G, Subramanian A. Growth factor and ultrasound-assisted bioreactor synergism for human mesenchymal stem cell chondrogenesis. *J Tissue Eng*. 2015;6. doi:10.1177/2041731414566529

20. Thakurta SG, Sahu N, Miller A, et al. Long-term culture of human mesenchymal stem cell-seeded constructs under ultrasound stimulation: Evaluation of chondrogenesis. *Biomed Phys Eng Express*. 2016;2(5). doi:10.1088/2057-1976/2/5/055016
21. Sahu N, Viljoen HJ, Subramanian A. Continuous low-intensity ultrasound attenuates IL-6 and TNFα-induced catabolic effects and repairs chondral fissures in bovine osteochondral explants. *BMC Musculoskelet Disord*. 2019;20(1):1-13. doi:10.1186/s12891-019-2566-4
22. Sahu N, Budhiraja G, Subramanian A. Preconditioning of mesenchymal stromal cells with low-intensity ultrasound: influence on chondrogenesis and directed SOX9 signaling pathways. *Stem Cell Res Ther*. 2020;11(1):1-15. doi:10.1186/s13287-019-1532-2
23. Petit B, Masuda K, D'Souza AL, et al. Characterization of crosslinked collagens synthesized by mature articular chondrocytes cultured in alginate beads: Comparison of two distinct matrix compartments. *Exp Cell Res*. 1996;225(1):151-161. doi:10.1006/excr.1996.0166
24. Tang et al. 2005. Three-dimensional Culture Systems to Induce Chondrogenesis of Adipose-Derived Stem Cells. *Bone*. 2008;23(1):1-7. doi:10.1007/978-1-61737-960-4
25. Hernandez PA, Jacobsen TD, Barati Z, Chahine NO. Confocal scanning of intervertebral disc cells in 3D : Inside alginate beads and in native microenvironment . *Jor Spine*. 2020;3(4):1-9. doi:10.1002/jsp2.1106
26. Cogswell PC, Kashatus DF, Keifer JA, et al. NF-κB and IκBα Are Found in the Mitochondria. *J Biol Chem*. 2003;278(5):2963-2968. doi:10.1074/jbc.M209995200
27. Subramanian A, Turner JA, Budhiraja G, Thakurta SG, Whitney NP, Nudurupati SS. Ultrasonic bioreactor as a platform for studying cellular response. *Tissue Eng - Part C Methods*. 2013;19(3):244-255. doi:10.1089/ten.tec.2012.0199
28. Murakami S, Lefebvre V, De Crombrugghe B. Potent inhibition of the master chondrogenic factor Sox9 gene by interleukin-1 and tumor necrosis factor-α. *J Biol Chem*. 2000;275(5):3687-3692. doi:10.1074/jbc.275.5.3687
29. Goldring MB, Marcu KB. Cartilage homeostasis in health and rheumatic diseases. *Arthritis Res Ther*. 2009;11(3). doi:10.1186/ar2592
30. Kanichai M, Ferguson D, Prendergast PJ, Campbell VA. Hypoxia promotes chondrogenesis in rat mesenchymal stem cells: A role for AKT and hypoxia-inducible factor (HIF)-1α. *J Cell Physiol*. 2008;216(3):708-715. doi:10.1002/jcp.21446
31. Ghosh S, May MJ, Kopp EB. NF-κB and rel proteins: Evolutionarily conserved mediators of immune responses. *Annu Rev Immunol*. 1998;16:225-260. doi:10.1146/annurev.immunol.16.1.225

Figures

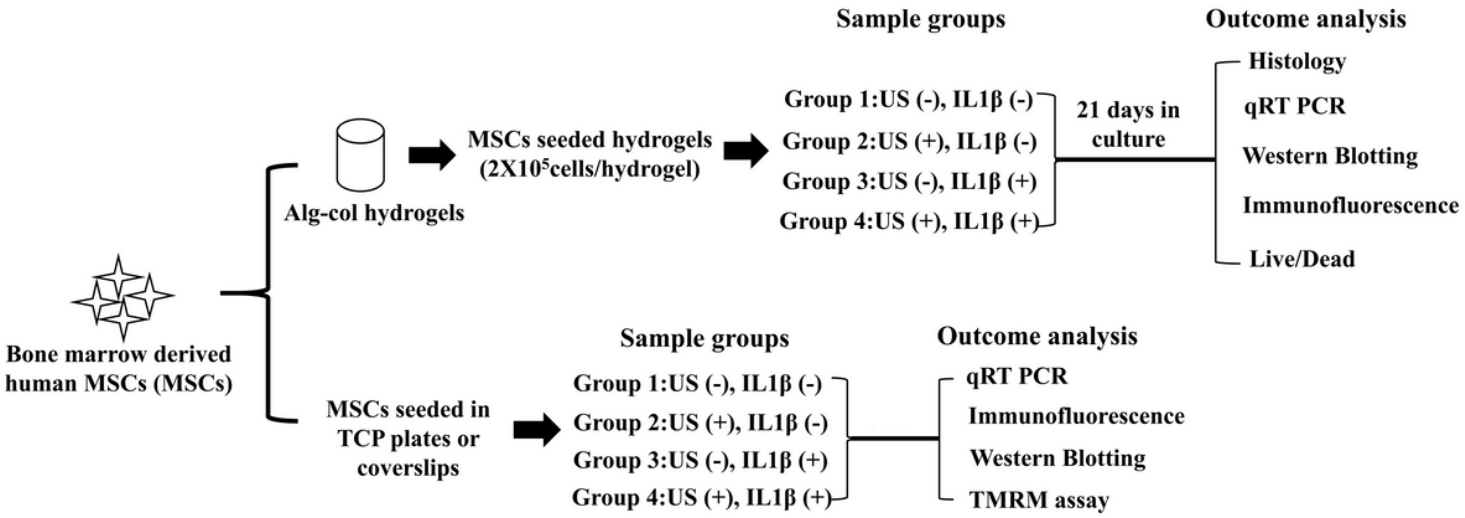

Figure 1

Experimental schematic. MSCs were seeded in alginate-collagen hydrogels or TCPs or coverslips and divided into groups as indicated. Group 1: cLIUS (-), IL1β (-); Group 2: cLIUS (+), IL1β (-); Group 3: IL1β (+), cLIUS (-) and Group 4: IL1β (+) cLIUS (+). Appropriate sample groups were treated with cytokine at a concentration of 10 ng/ml. cLIUS stimulation was applied as follows:14 kPa (5.0 MHz, 2.5 Vpp), and 10 or 20 min /application. Non-cytokine treated and non-cLIUS stimulated samples served as controls. Upon completion of the study, samples were retrieved and subjected to the indicated outcome analyses.

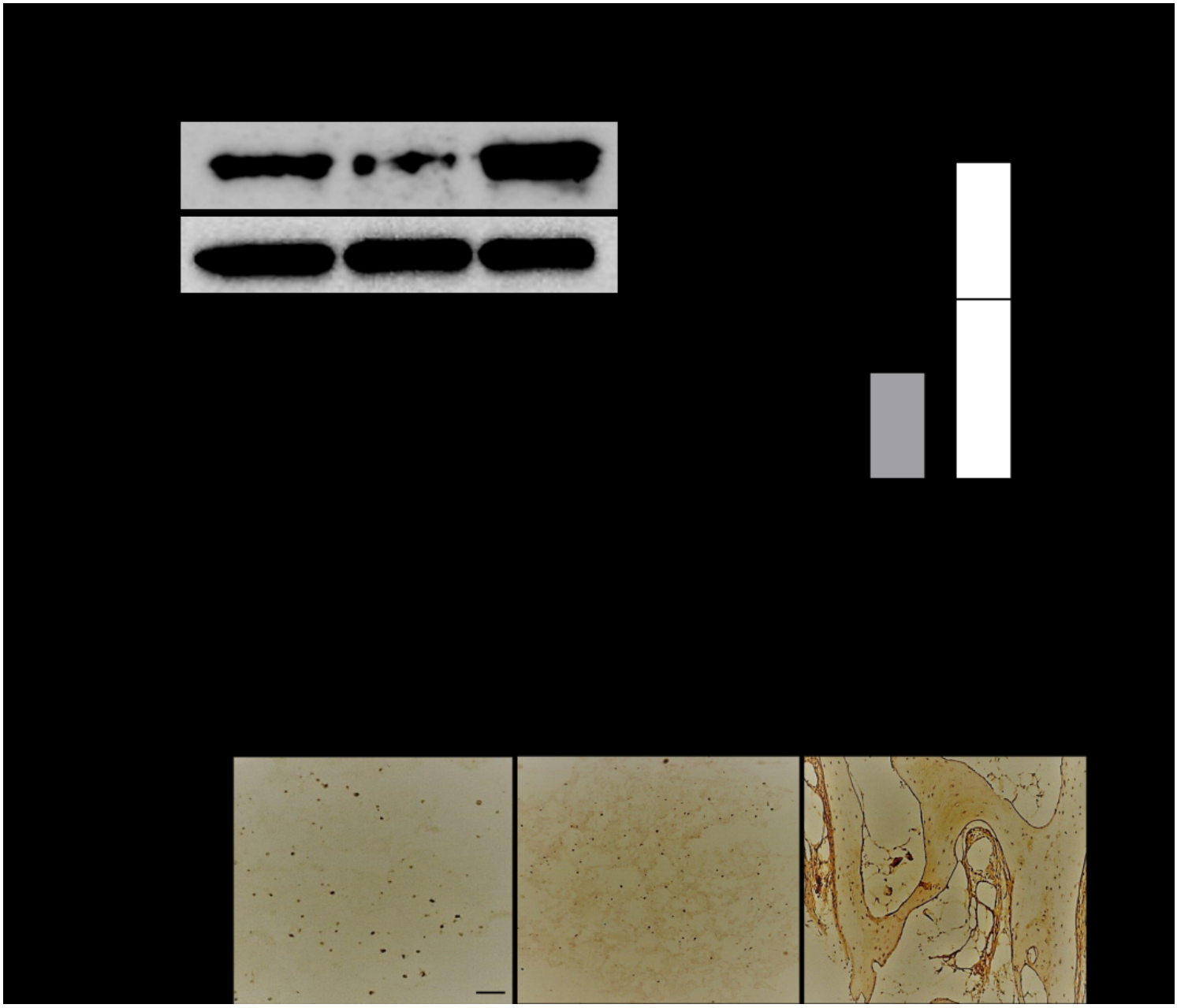

Figure 2

Protein analysis of Collagen II by western blotting and immunohistochemical staining. Scaffolds were retrieved on day 21 and processed for western blotting and immunohistochemical staining, respectively. (A) Detection of COLII protein expression by western blotting and β-actin was used as a loading control. (B) Blots were quantified using ImageJTM software and presented. (C) Representative images of sections (8 μm) stained for COLII, and a human bone section was included as a positive control. Data are shown as the mean ± standard deviation of samples; p-value represents statistical significance (p*< 0.05; p** < 0.01; p***<0.001 and p****<0.0001).

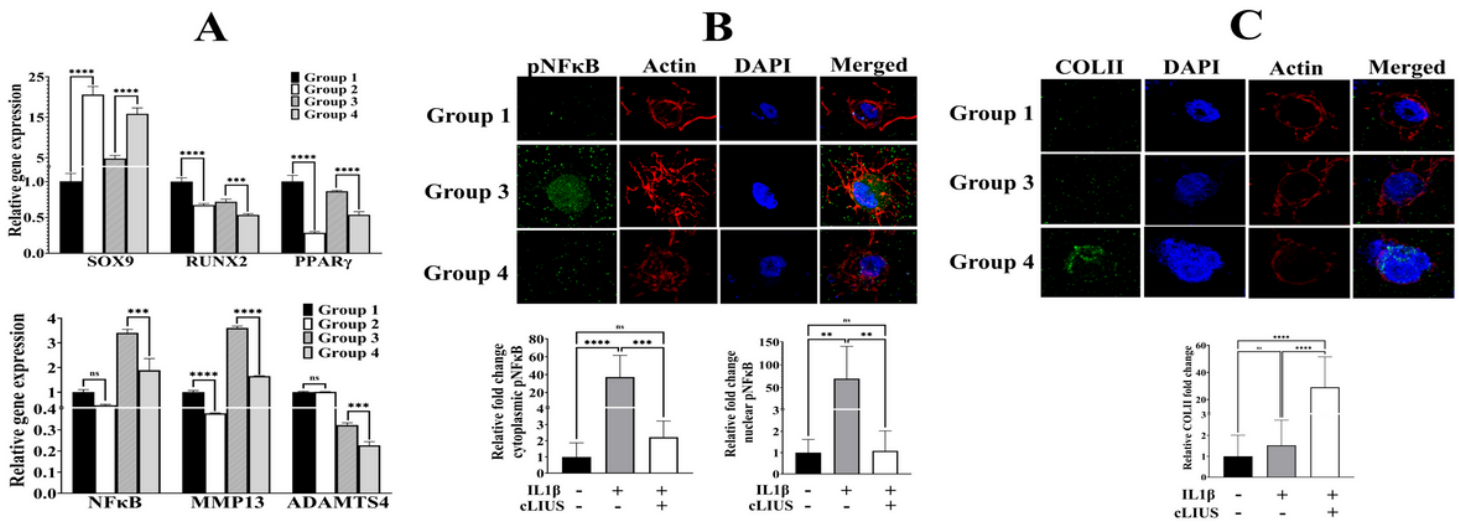

Figure 3

Gene expression analysis and localization of pNFκB and COLII in hydrogel scaffolds: At the end of 21 days of culture, hydrogels were subjected to both gene expression and IF analysis. Briefly, cell homogenates (n=10) were prepared from hydrogels, and total RNA was extracted, and gene expression of lineage markers and catabolic markers was evaluated by qRT-PCR, and GAPDH was used as a housekeeping gene (A). Hydrogels were fixed using 4% PFA in HBSSCM and stained against pNFκB and COLII (green fluorescence), respectively, in separate experiments (B, C), and nuclei were counter stained with DAPI (blue fluorescence). Z stacks of the hydrogels were captured using the Zeiss LSM 700 confocal microscope with 63x magnification (z step size 5µm), and fluorescence intensity was quantified using ImageJTM software (n=15). Data are shown as the mean ± standard deviation of samples and p-value represents statistical significance (p*< 0.05; p**< 0.01; p***<0.001 and p****<0.0001).

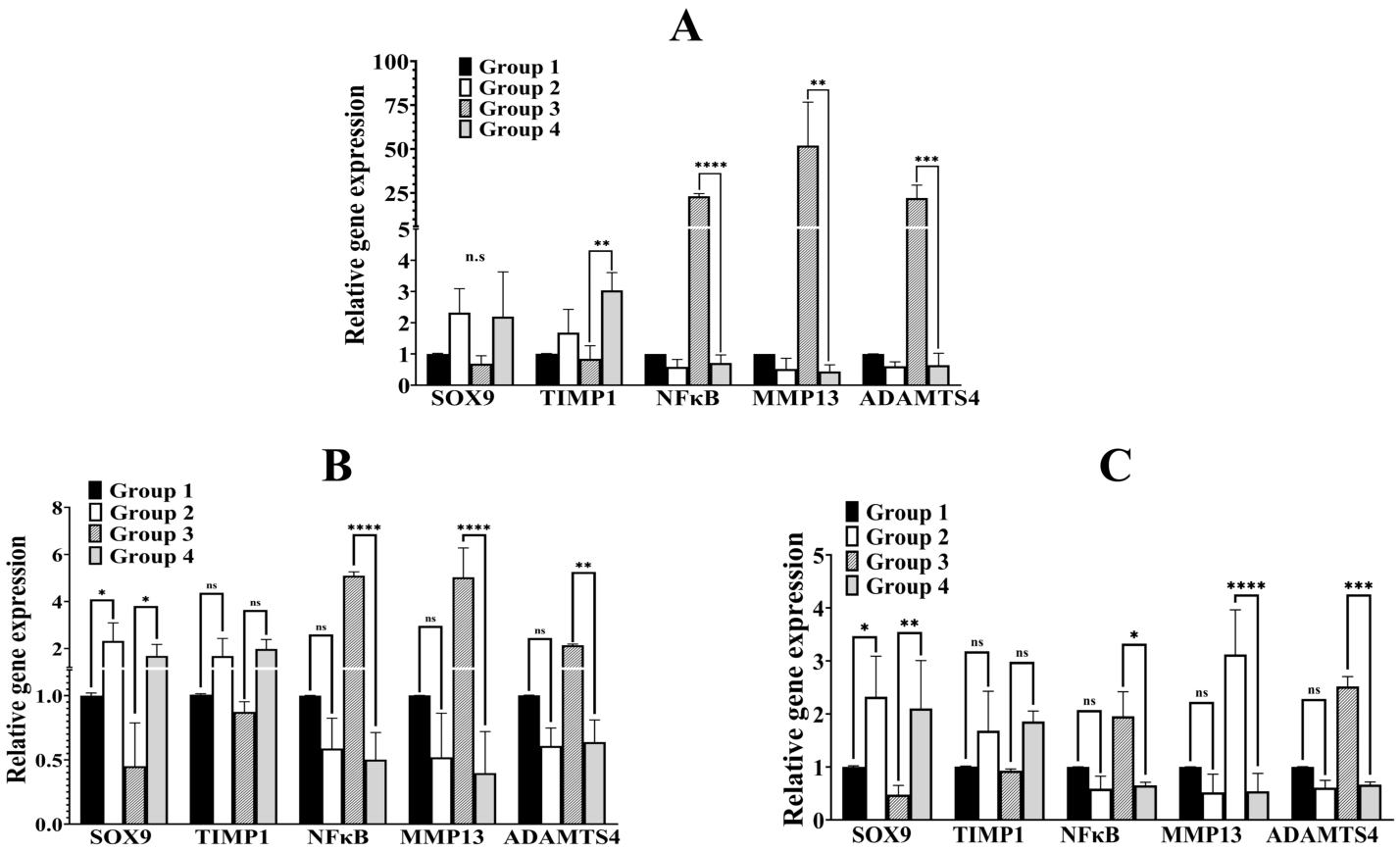

Figure 4

Gene expression analysis in MSCs exposed to IL1β(A), TNFα(B) and IL6(C). MSCs were seeded on TCPs and treated as depicted in Figure 1. Homogenates from two wells per group served as one replicate and three such replicates were used for gene expression analysis (n = 3). Total RNA was extracted, and the gene expression of anabolic and catabolic markers was evaluated by qRT-PCR and GAPDH was used as a housekeeping gene. Bar graph represents mean ± 95% confidence interval; p values indicate statistically significant differences (p*< 0.05; p**< 0.01; p***<0.001 and p****<0.0001).

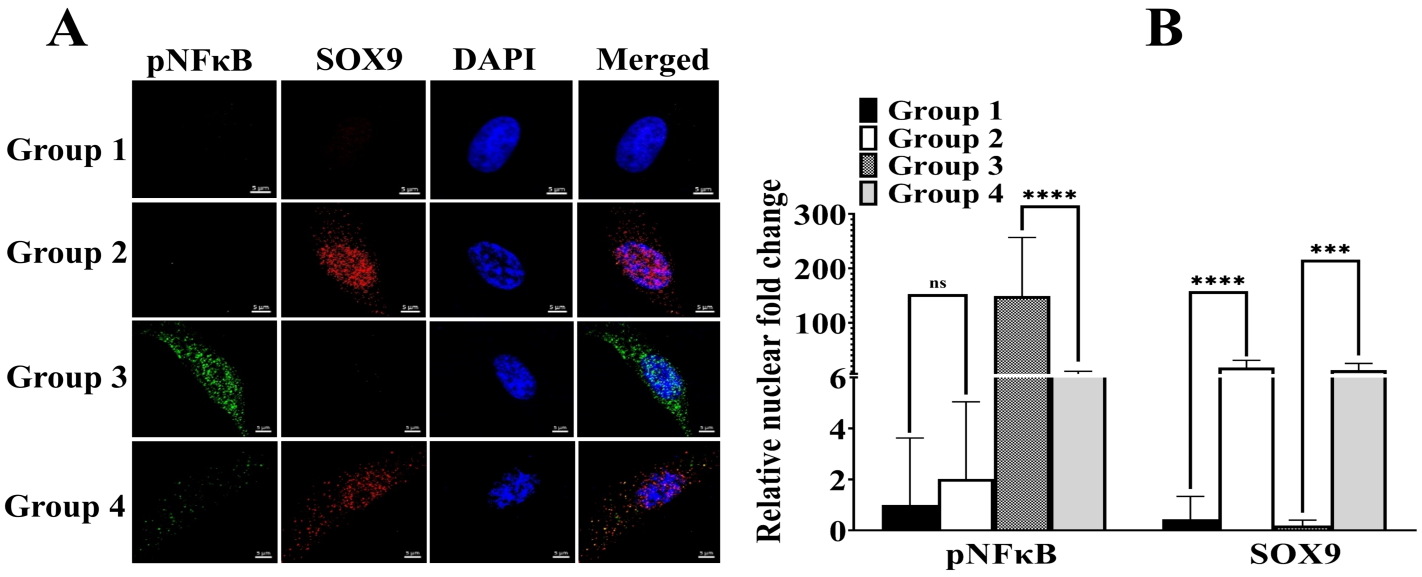

Figure 5

Localization of SOX9 and pNFκB in MSCs exposed to IL1β. MSCs were seeded on coverslips and treated as depicted in Figure 1. Coverslips were fixed and double stained for pNFκB (green fluorescence) and SOX9 (red fluorescence) antibodies, and nuclei were counter stained with DAPI (blue fluorescence). (A) Images were captured using 63x magnification and presented. (B) Fluorescence intensity was quantified using ImageJTM software (n=30). Bar graph represents mean ± 95% confidence interval; p values indicate statistically significant differences. (p*< 0.05; p**< 0.01; p***<0.001 and p****<0.0001) and the scale bar represents 5µm.

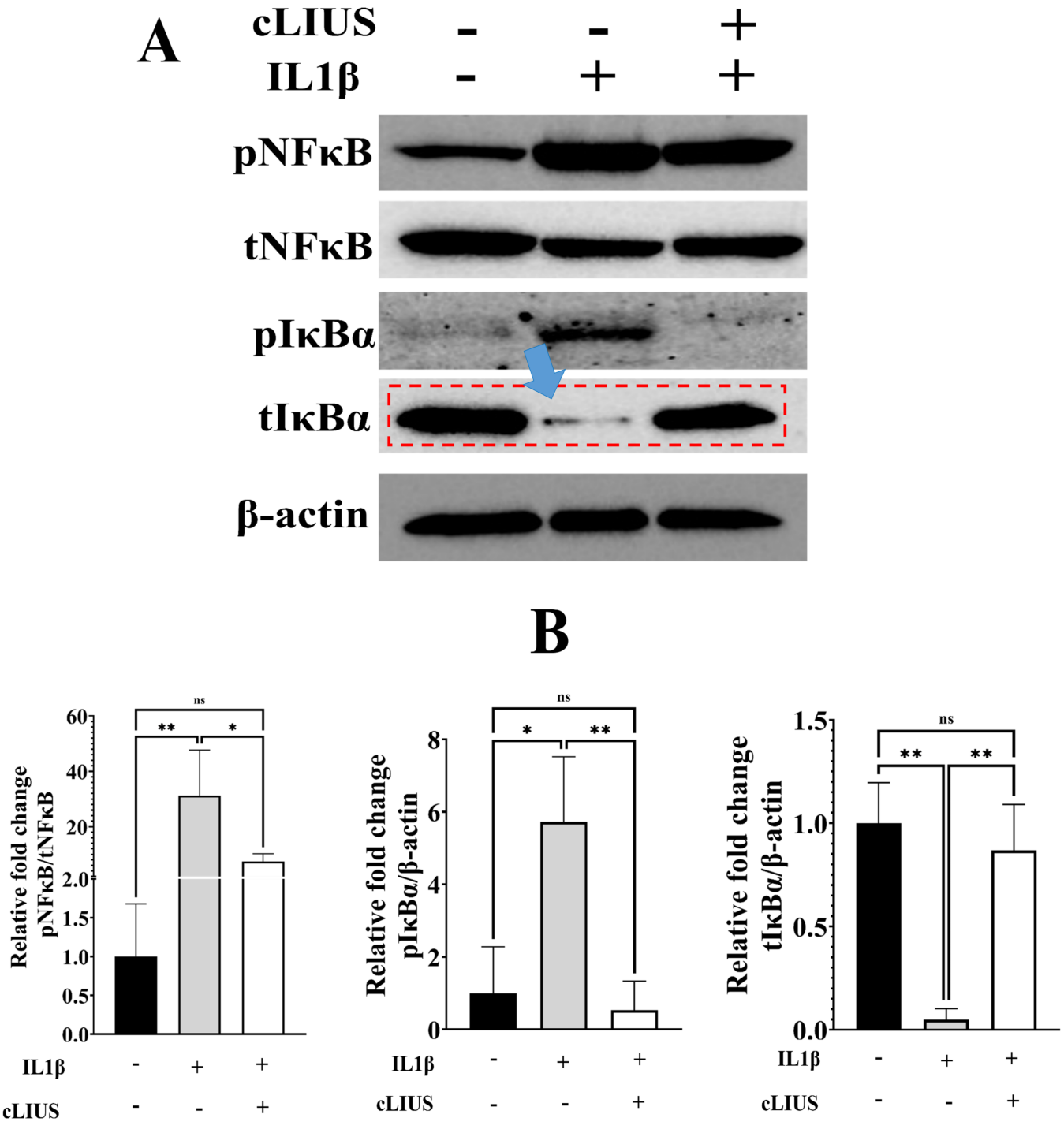

Figure 6

Phosphorylation of NFκB and IκBα. MSCs were seeded on TCP plates and treated as depicted in Figure 1. Total cell lysates were obtained and analyzed by western blotting using specific antibodies. (A) Protein expression of phospho-NFκB total NFκB, phospho-IκBa total IκBa in indicated samples by western blotting, and β-actin was used as a loading control. (B) Blots were quantified using ImageJTM software and presented. Data are shown as the mean ± standard deviation of samples in duplicate; p-value represents statistical significance (p*< 0.05; p** < 0.01; p***<0.001 and p****<0.0001).

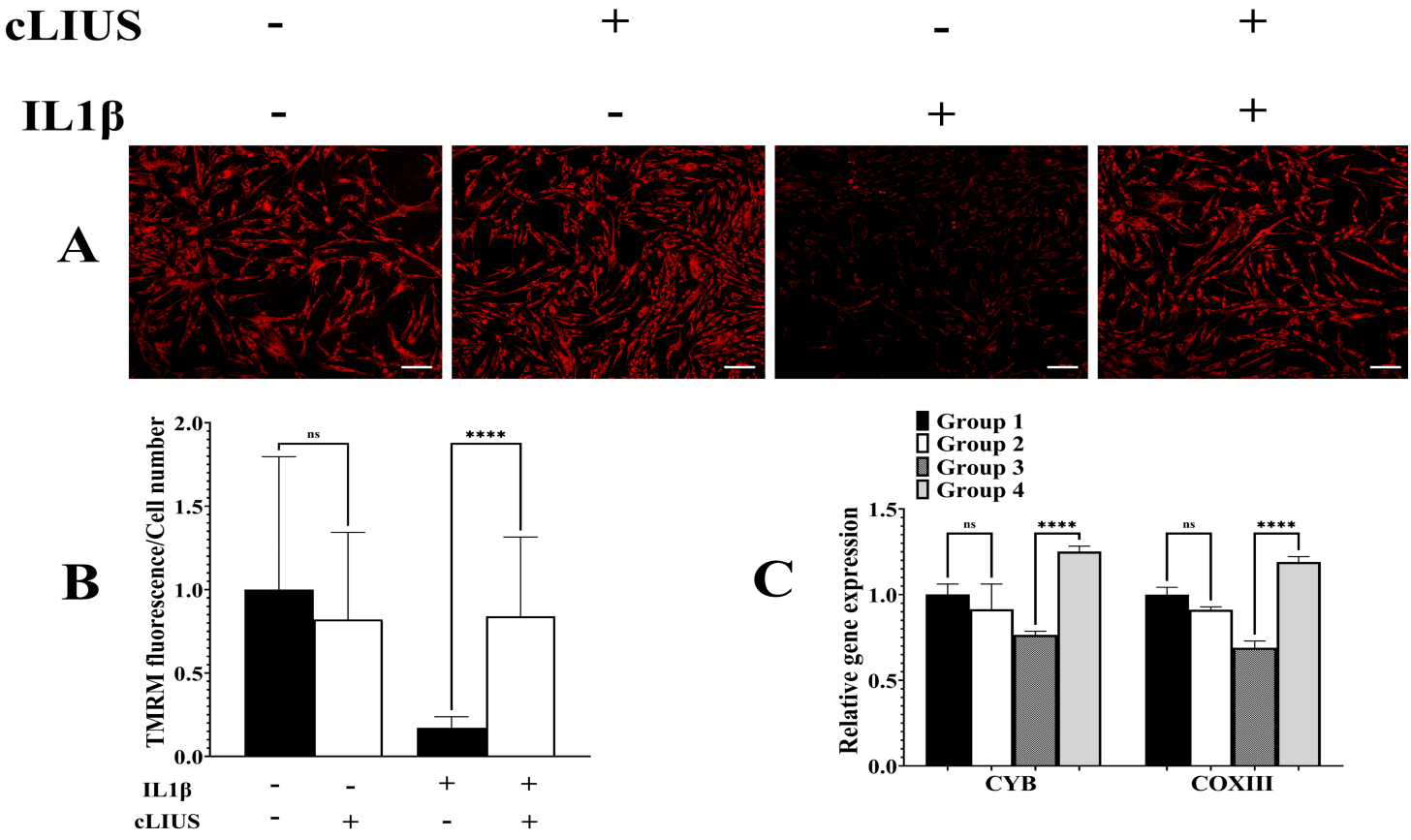

Figure 7

Assessment of mitochondrial potential and mRNA expression under cLIUS. MSCs were seeded on coverslips and treated as depicted in Figure 1. Coverslips were treated with 100nM TMRM reagent for 30 minutes and live images were captured using the Zeiss LSM 700 confocal microscope and images are presented (A). Fluorescence data was quantified (n=50) using ImageJTM software and the fluorescence intensity graph presented (B) along with mitochondrial gene expression (C). All data shown as the mean ± standard deviation of samples and p-value represents statistical significance (p*< 0.05; p** < 0.01; p*** <0.001 and p****<0.0001), and scale bar represents 100μm.

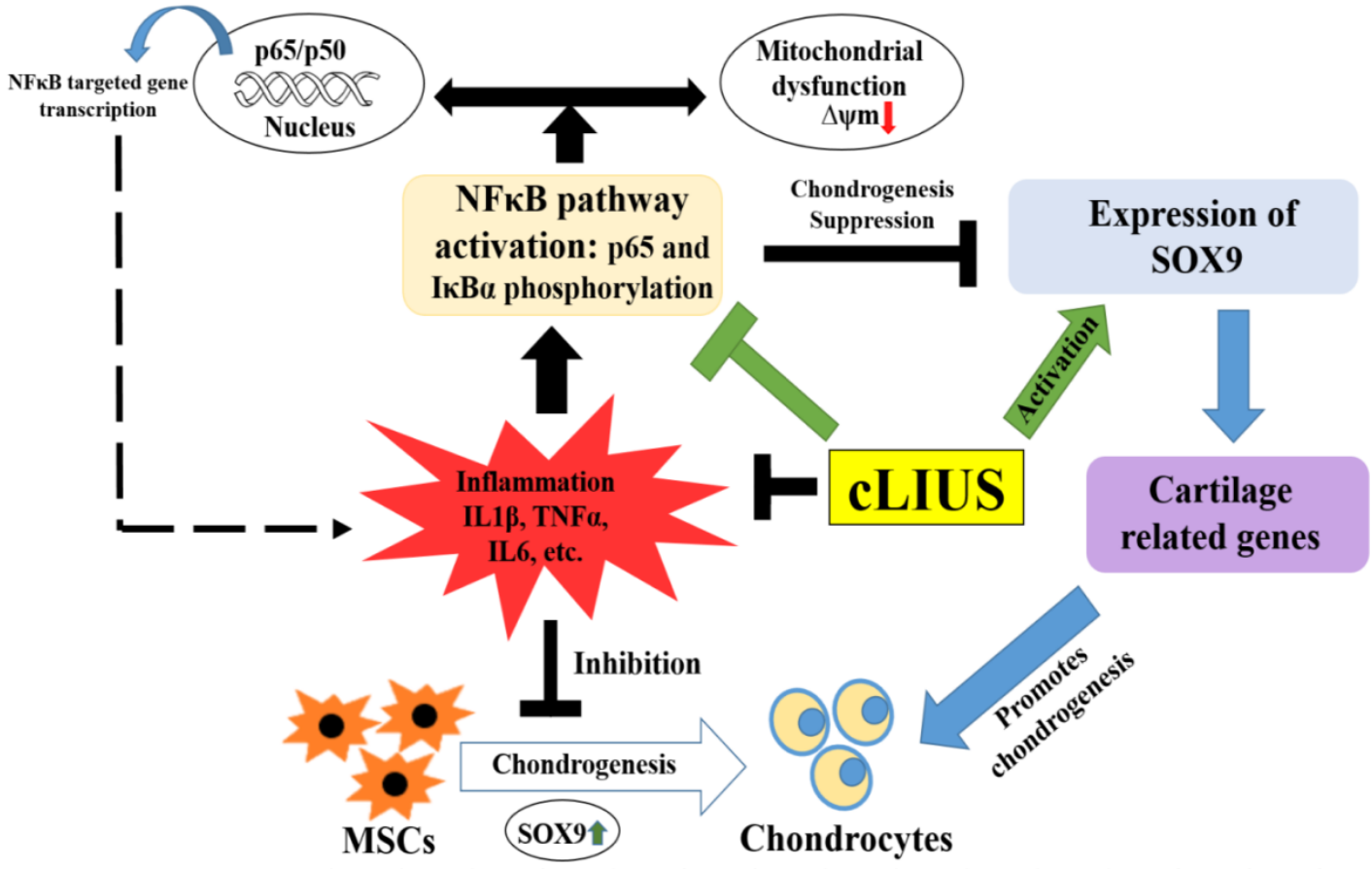

Figure 8

Schematic representation of the cLIUS induced chondroprotective mechanisms. cLIUS promoted MSC chondrogenesis by inhibiting the cytokine-induced activation of the NFκB signaling pathway by engaging the tIκBα feedback mechanism while upregulating the expression of SOX9, the collagen II transcription factor. It is also posited that cLIUS acts to preserve the mitochondrial potential, which is impacted by cytokines.

Supplementary Files

This is a list of supplementary files associated with this preprint. Click to download.

- Additionalfile1FigureS1.tiff
- Additionalfile2FigureS2.tiff
- Additionalfile3FigureS3.tiff